Available online at www.elixirpublishers.com (Elixir International Journal)

Digital Processing

Elixir Digital Processing 88 (2015) 36137-36155

ISSN: 2229-712X

A Comparison of Two Kidney Stone Segmentation Techniques

R. B. Dubey and Anju Dahiya

Hindu College of Engg, Sonepat, Haryana, India.

ARTICLE INFO

Article history:

Received: 22 September 2015;

Received in revised form:

28 October 2015;

Accepted: 03 November 2015;

Keywords

Kidney stone,
Segmentation,
Electromagnetism optimization algorithm,
Harmony search algorithm.

ABSTRACT

Kidney stone disease is very common among Indians and approximately 5-7 million patients suffer from stone disease. The most popular imaging modality for its treatment is ultrasound imaging. Segmentation accuracy determines the eventual success or failure of computerized analysis procedures. Traditional methods available for segmentation of kidney stones are not accurate. We use the evolutionary techniques for segmentation of the kidney stone ultrasound images for the first time based on electromagnetism optimization algorithm and harmony search algorithm for determining multilevel threshold of images. In most cases, the optimal thresholds are found by the minimizing or maximizing an objective function, which depends on the positions of the thresholds. We identify a class of objective functions for which the optimal thresholds can be found using algorithms with low time complexities. The Kapur's entropy function and Otsu's between class variance is maximized using these algorithms and an optimal threshold values at different levels are found out. The area of extracted stone is calculated and compared with the area given by the expert radiologist. The other metric used to compare the segmented image and the original image is the peak signal to-noise-ratio (PSNR) value. The relative error is also calculated to show the segmentation accuracy of each method.

Introduction

The ultrasound imaging is the most popular and cost effective imaging modality for treatment of kidney stone disease. Image segmentation is the low level image processing technique which aims to partition an image into regions such that each region groups pixels sharing similar attributes. Segmentation of nontrivial images is one of the most difficult tasks in image processing. Segmentation accuracy determines the eventual success or failure of computerized analysis procedures. For this reason, considerable care should be taken to improve the probability of accurate segmentation. Here we segment the image and detect the stones present in kidney. Individual errors may occur during the interpretation of ultrasound image by an untrained sonographer, while taking dimensions. Thus, for the purpose of avoiding the dependability to the sonographers' expertise, some image processing operations are applied for segmentation and detection of stone. We use the evolutionary techniques for segmentation of the kidney stone ultrasound images based on electromagnetism optimization algorithm and harmony search algorithm for determining multilevel threshold for image.

Segmenting the calculi from the kidney images is very useful for the medical diagnosis in analyzing the patient's data. Considering the importance of the kidney stone segmentation, many research works are developed with different techniques to accomplish the kidney stone segmentation process. This work focuses on the detection of kidney stone using segmentation approaches which uses the ultrasound kidney image as input. The ultrasound images are very challenging and prone to speckle noise so images are pre-processed firstly using the image restoration methods and then segmented by the proposed segmentation approaches. Afterwards, the stone is extracted and the area of the detected stone is compared to calculate the error and accuracy of methods used [14, 16].

The remainder of this paper is organized as follows. Section 2 reviews the relevant previous literature and highlights the research motivation. Section 3 presents the materials and data set used. Section 4 summarizes the details of methodology. Section 5 provides results and discussions. Conclusions are drawn in Section 6.

Related Work

Kidney stone disease is very prevalent among Indians out of every 1000 Indian 3 people are suffering from kidney stone. The problem of stone can be due to various reasons such as food habits, salts present in drinking water and it could be genetic. Ultrasound imaging modality is one of popular method used by specialist to diagnose it. The reason behind the wide use of ultrasound images is because they are non-invasive, portable, radiation free, and affordable. Segmentation helps to detect and analyze the images which provide useful information regarding the progress of the disease [14]. The presence of speckle noise in ultrasound images is a problem which requires preprocessing of images before segmentation [13, 14, 16]. Normally, segmentation process is based on the image gray-level histogram, namely image histogram thresholding. The threshold based methods are parametric and non-parametric types. In parametric approaches, it is necessary to find some parameters like probability density function which models each class and these approaches are time consuming and computationally complex. Whereas the non-parametric involves use of several terms like between class variance, entropy, error rate etc. which is needed to be optimized to find an optimal threshold values. For bi-level thresholding the classical methods are Otsu method which chooses the optimal thresholds by maximizing the between class variance of gray levels and Kapur's method finds the optimal threshold values by maximizing the entropy of histogram. Multilevel thresholding uses a number of thresholds in the histogram of the image to separate the pixels of the objects in the image. Although both Otsu and Kapur's method can be expanded to multilevel thresholding but the problem lies in the selection of the optimal thresholds due to computational complexity which increases exponentially with

Tele: 9971833006
E-mail addresses: rbdubeyster@gmail.com

each new threshold. To solve the optimization problem efficient search or optimization algorithms are needed. To eliminate such problems evolutionary techniques have been applied in solving multilevel thresholding problems. These are non-deterministic algorithms like genetic algorithms (GA), ant colony optimization (ACO), particle swarm optimization (PSO) and electro-magnetic optimization (EMO) have been successfully applied to multilevel thresholding problem. These are the forms of probabilistic heuristic algorithm. Genetic algorithm method is generally faster and has been successfully employed to solve complex non-linear problems but research has identified some deficiencies in GA performance [26]. EMO method can also be employed over multilevel thresholding problem and it is finding to exhibit low computational overhead. BFO is also one of nature inspired algorithm can be used to optimize multilevel thresholding problems. BFO is used to segment the ultrasound images of kidney stones using Otsu and Kapur as objective function [4].

Evolution is the process which forces the organisms to adapt with nature and those who fail to adapt are eliminated or we can say the best fittest one can survive. This behavior of organisms motivated scientist to use these evolutionary principles to hypothetically develop such model which can be optimized to find best value. Foraging theory assumes that organisms search for and obtain nutrient in a way that maximizes energy intake E per unit time T. The foraging behavior of E.coli bacteria can be mimicked to hypothesize a model which can be used for optimization to find best value. Firstly Passino in 2002 developed an algorithm which utilizes the foraging behavior of E.coli bacteria. The algorithm is divided into four parts chemotaxis, swarming, reproduction, elimination and dispersal. The bacterial foraging optimization algorithm requires specification of a variety of parameters [1].

Several hybrid approaches are also employed whose primary objective is to cluster chunks of data by using simplistic collaboration. The hybrid approach for clustering based on particle swarm optimization (PSO) and bacteria foraging algorithm (BFA) developed a new method auto CPB (Auto-clustering based on particle bacterial foraging).GA in combination with K-means clustering algorithm develops an improved K-means clustering algorithm based on improved initial focal point and K-value determination which improved clustering algorithm stability more efficiently [11, 27].

Electromagnetism mechanism algorithm is one of the best optimization algorithms which are based on the attraction and repulsion behavior of the charged particles in the electromagnetic field. This algorithm has better performance in the optimal solution accuracy and the average solution time [16]. Another work is based on thresholding of images using social impact theory based optimization (SITO) is an algorithm based on human behavior. In case of bi-level thresholding the cross entropy function works well but for multilevel thresholding a global and generic objective function is needed and on the basis of statistical measures such as standard deviation, entropy, MSE, PSNR values, SITO performs better [18]. A work introduces a new color space for facial skin segmentation and its features and advantages and BFO is used to optimize objective function. To perform thresholding, the entropy-based method is applied and the BFO algorithm is used to optimize the threshold value [12]. GA combined with adaptive neuro- fuzzy inference system (ANFIS) provides improved accuracy, sensitivity, specificity for the segmentation of brain tumor from MRI Images. ANFIS is an adaptive network which provides benefits of both fuzzy and neural network [13]. Automatic segmentation and right number of segments of human normal and abnormal MR brain images can be estimated by a combination of a GA and the fuzzy C-means method. The fitness function is calculated using FCM which is used in GA to perform segmentation [14]. Ultrasound images have low contrast and contain speckle noise. It can make the detection of kidney abnormalities such as stones, cysts, cancerous cells, congenital anomalies, blockage of urine a challenging task. Due to which preprocessing of images is carried out to remove speckle noise. Preprocessing of ultrasound images may include restoration to reduce speckle noise then for image smoothening Gabor filter may be applied. Also image can be enhanced using histogram equalization. Over preprocessed image segmentation technique like level set segmentation can be applied [18]. Genetic algorithm is helpful in finding optimal feature vectors and to identify an approximate global optimal region in medical image segmentation [20]. Improved genetic algorithm in which probability ties of crossover are varied with respect to individual ranking instead of fitness function is found to have reduced operating time [21]. The various challenges of medical image segmentation arise due to poor image contrast and artifacts that result in missing or diffuse organ/tissue boundaries. Also search space is often noisy with a multitude of local optima. GA is found to be effective in coming out of local optima thus brings out as a better approach for segmentation [19].

Region indicator with contour segmentation method has five major steps which includes selection of exact calculi from renal calculi image. Image is enhanced using histogram equalization and most interested pixel values are selected using K- means clustering. In final stage a number of regions are selected. Also use of ANFIS makes the techniques more efficient [17]. The method proposed was based on improved seeded region growing which can perform both segmentation and classification of kidney stone images. The images can be classified as normal stone, early stone stage by recognizing multiple classes. Homogenous region of image are found to be relied on the image granularity features in the enhanced semiautomatic SRG based image segmentation process, in which the pertinent structures with dimensions similar to the speckle size extracted. The high frequency artifacts are being reduced by performing region merging after the region growing [20].

Ultrasound scanning of kidney is done to asses kidney size, shape, location to detect whether there is any abnormalities like cysts, and stones are present or not. A method of automatic region of interest generation is proposed for kidney ultrasound images. The method consists of the speckle noise reduction using Gaussian low pass filter, calculation of local entropy of image, threshold selection, morphological operations, object windowing, determination of seed point and ROI generation [14]. Performance of segmentation algorithms such as Otsu, K-means and FCM have evaluated on the basis of segmentation rate and segmentation time. In terms of segmentation time Otsu is found to be faster than others. Segmentation rate of K-means is observed to be 90% better over X-ray images [15]. The method proposed uses two important steps classification and segmentation. The image preprocessing includes contrast enhancement which is improved by using histogram equalization and reference pixel are selected via GA techniques. The ANFIS system is used for the training and classification of ultrasound images. Images of manually segmented stone regions are used by ANFIS system. During the testing process, the reference and test images are compared and morphological dilation operation is performed [19].

3-D ultrasound kidney images have found a wide scope for diagnosis of kidney stones patients. A new automated kidney detection approach using 3-D Morison's pouch ultrasound images is proposed. The probabilistic kidney shape model is generated to estimate the probable shape of kidney. Then preprocessing steps are performed to remove the speckle noise and low contrast of images. For this purpose a 3-D finite impulse response filter can be used which is followed by the histogram equalization process. Histogram equalization operates as a global transformation and is not able to capture local intensity condition of the entire image. Thereafter segmentation of kidney stone image is performed [23].

Based on fuzzy partition and maximum correlation criterion a new image histogram thresholding method is proposed. Regions such as object and background of the images are considered ambiguous in nature therefore regions are transformed into fuzzy domain with membership functions. Differential evolution method is found to have good search ability [24]. The work proposed describes a semiautomatic technique for segmentation of kidney from ultrasound images by using seeded region growing technique (SRG). The proposed SRG is found to perform better than conventional segmentation algorithms and analysis is based on various statistical measures [26].An improved adaptive tumbling bacterial foraging optimization (ATBFO) performed the lowest fitness function and fastest practice which is concerned to solve the non- convex and complexity issues of solving economic dispatch issues [23].

In harmony search (HS) algorithm, each solution is called a harmony and is represented by an n-dimension real vector. An initial population of harmony vectors are randomly generated and stored within a harmony memory (HM). A new candidate harmony is then generated from the elements in the harmony by using a memory consideration operation either by a random re-initialization or a pitch adjustment operation. Finally, the harmony memory is updated by comparing the new candidate harmony and the worst harmony vector in the harmony memory. The worst harmony vector is replaced by the new candidate vector when the latter delivers a better solution in the harmony memory. The above process is repeated until a certain termination criterion is met. The basic harmony search algorithm consists of three main phases: initialization, improvisation, and updating [21]. In addition, the HS algorithm is a population-based meta-heuristic, meaning that multiple harmonics groups can be used in parallel. Proper parallelism usually leads to better implantation with higher efficiency [24].

Image database

The data is collected from the Cygnus J.K. Hindu Hospital, Industrial area, Sonepat, Haryana, India. The database contains 20 ultrasound images of kidney stone which are marked by the expert radiologist so that after applying the proposed methodology the extracted stone area can be compared to test the accuracy of the proposed algorithms. The software tool applied for the purpose of work is MATLAB version 8.1.0 (R2013a).

Proposed Methodology

Image segmentation is a process of dividing an image into different regions. One of the basic types of segmentation is thresholding. The segmentation approach used here is multilevel thresholding technique. It is one of the most widely used image segmentation operations; one application is foreground-background separation. Thresholding is used to extract an object from its background by assigning an intensity value T (threshold) for each pixel such that each pixel is either classified as an object point or a background point. For gray scale images, thresholding is widely considered to extract key features from input image. The main objective is to enhance the key feature of an image using the best possible bi-level as well as the multilevel threshold. The nonparametric classical segmentation procedures such as Otsu, Kapur, and Kittler are very efficient and successful in the case of bi-level thresholding process [3]. When the number of threshold level increases, classical thresholding techniques require more computational time. Hence, heuristic methods based bi-level and multi-level image thresholds have increased the interest of researchers for better computational efficiency.

Multilevel thresholding is the extension to segmentation into more than two classes. To find the thresholds, which separate the classes, the histogram of the image is analyzed. In most cases, the optimal thresholds are found by the minimizing or maximizing an objective function, which depends on the positions of the thresholds. Evolutionary algorithms are search and optimization techniques inspired by nature, have been broadly applied to solve multi-objective optimization problems. Optimization means finding the best possible solution. Median filter can remove the high frequency components from ultrasound images without disturbing the edges. A median is calculated by sorting all pixel values by their size, then selecting the median value as the new value for the pixel. For each pixel, 5*5 windows of neighborhood pixels are extracted. Initially the pixel intensity values are arranged in ascending order and the median value is calculated and the center pixel is replaced with the median value.

Thresholding

Otsu method

The Otsu method is a popular non-parametric method in medical image segmentation.

Let the intensity of gray level image be expressed in L gray-level [1, 2, 3.....L]. The number of points with gray level at i is denoted by $h(i)$ and the number of points can be expressed as N = $x_1 + x_2 + x_3 + \ldots\ldots\ldots + x_L$. The histogram of this gray level image be regarded as an occurrence of distribution of probability

$$p(i) = \frac{h(i)}{N}, \quad h(i) \geq 0, \quad \sum_{i=1}^{L} p_i = 1, \tag{1}$$

Image pixels are divided into two parts C_0 and C_1 i.e., foreground and background by a threshold t. Where C_0 represents pixels within levels [1, 2, 3,.....,t], and C_1 denotes pixels within levels [t+1,.....,L]. The occurrence probabilities of this class and average can be expressed as respectively

$$\omega_0 = \omega(t) = \sum_{i}^{t} p(i) \tag{2}$$

$$\omega_1 = 1 - \omega(t) = \sum_{i=t+1}^{L} p(i)$$

$$\mu_0 = \sum_{i=1}^{t} \frac{i.p(i)}{\omega_0} = \frac{1}{\omega(t)} \sum_{i=1}^{t} i.p(i) \tag{3}$$

$$\mu_1 = \sum_{i=t+1}^{L} \frac{i.p(i)}{\omega_1} = \frac{1}{1-\omega(t)} \sum_{i=t+1}^{L} i.p(i)$$

Total mean can be expressed as:

$$\mu_T = \sum_{i=1}^{L} i.p(i) \tag{4}$$

and we can find that:

$$\mu_T = \mu_0\omega_0 + \mu_1\omega_1 \tag{5}$$

where ω_0 and ω_1 are the probabilities of foreground and background parts. Besides the μ_0, μ_1 and μ_T are the mean of foreground part, background part and the entire grayscale image respectively. The between class variance σ_B^2 of the two classes C_0 and C_1 is given by:

$$\sigma_B^2 = \omega_0(\mu_0 - \mu_T)^2 + \omega_1(\mu_1 + \mu_T)^2 \tag{6}$$

The separable degree η of the class, in the discrimination analysis is:

$$\eta = \max_{1\le t\le L} \sigma_B^2 \tag{7}$$

Finally maximizing σ_B^2 to choose to choose the optimal threshold t^*

$$t^* = \arg\max_{1\le t\le L} \sigma_B^2 \tag{8}$$

Thus the objective function can be defined as:

$$MaximizeK(t) = \sigma_0 + \sigma_1 \tag{9}$$

$$\sigma_0 = \omega_0(\mu_0 - \mu_T)^2 \text{ and}$$

$$\sigma_1 = \omega_1(\mu_1 - \mu_T)^2 \tag{10}$$

The optimal threshold is the gray level that maximizes the between class variance.

The above used method is for bi-level thresholding but it can be easily extended to multilevel thresholding of an image. Let there are M thresholds in an image such that $\{t_1, t_2, \ldots\ldots\ldots, t_{M-1}\}$ which divides the original image into M+1 classes. C_1 for $[1,\ldots\ldots,t_1]$, C_2 for $[t_1 + 1,\ldots\ldots,t_2]$,....., C_i for $[t_{i+1} +1,\ldots\ldots t_i]$,.....,and C_{M+1} for $[t_M +1,\ldots,L]$, the optimal thresholds $\{t_1^*, t_2^*, \ldots\ldots\ldots, t_M^*\}$ are obtained by maximizing σ_B^2 as:

$$\{t_1^*, t_2^*, \ldots\ldots\ldots, t_M^*\} = \arg\max_{1\le t_1<\ldots\ldots<t_M<L} \{\sigma_B^2(t_1, t_2, \ldots t_M)\} \tag{11}$$

where

$$\sigma_B^2 = \sum_{k=1}^{M} w_k(\mu_k - \mu_T)^2 \tag{12}$$

The objective function can be defined as:

$$\text{Maximize } K(t) = \sigma_0 + \sigma_1 + \ldots\ldots\ldots + \sigma_M \tag{13}$$

where

$$\sigma_0 = \omega_0(\mu_0 - \mu_T)^2$$

$$\sigma_1 = \omega_1(\mu_1 - \mu_T)^2$$

$$\sigma_M = \omega_M(\mu_M - \mu_T)^2 \tag{14}$$

Kapur entropy method

Kapur's entropy method is based on maximizing the entropy measure of the segmented histogram such that each separated region has a more centralized distribution. The entropy of an image measures the compactness and separability among classes [2]. This method of thresholding is also developed primarily for bi-level thresholding but can be extended to multilevel thresholding. Consider an image and let L be the gray levels of the given image, these gray levels are in the range {1, 2,.....L}. Then the probability distribution can be defined as

$$P_i = \frac{h(i)}{N}, \text{ for } (0 \le i \le L) \tag{15}$$

where $h(i)$ is the number of pixels for the corresponding gray level L, N is the total number of pixels in the image.

The entropy of the background and foreground parts can be defined as:

$$H_0 = -\sum_{i=1}^{t} \frac{P_i}{\omega_0} \ln \frac{P_i}{\omega_0}, \quad \omega_0 = \sum_{i=1}^{t} P_i \text{ and}$$

$$H_1 = -\sum_{i=t+1}^{L} \frac{P_i}{\omega_1} \ln \frac{P_i}{\omega_1}, \quad \omega_1 = \sum_{i=t+1}^{L} P_i \tag{16}$$

Thus the objective function can be defined as:

$$\text{MaximizeK(t)=H}_0\text{+H}_1$$

Similarly, it can be extended to the optimal multilevel thresholding problem, it can be defined as a M dimensional optimization problem which results M optimal thresholds for a given image [$t_1, t_2, t_3, \ldots\ldots t_M$] so the objective function is defined as:

$$\omega_M = \sum_{i=t_M+1}^{L} P_i \tag{17}$$

where

$$H_0 = -\sum_{i=1}^{t} \frac{P_i}{\omega_0} \ln \frac{P_i}{\omega_0}, \quad \omega_0 = \sum_{i=1}^{t} P_i$$

$$H_1 = -\sum_{i=t+1}^{L} \frac{P_i}{\omega_1} \ln \frac{P_i}{\omega_1}, \quad \omega_1 = \sum_{i=t+1}^{L} P_i$$

$$H_M = -\sum_{i=t_M+1}^{L} \frac{P_i}{\omega_M} \ln \frac{P_i}{\omega_M}, \quad \omega_M = \sum_{i=t_M+1}^{L} P_i \tag{18}$$

Electromagnetism-like optimization algorithm

A solution in electromagnetism like algorithm is the charged particle in search space and this charge is related to the objective function value. Electromagnetic force exists between two particles. With the force, the particle with more charge will attract the other while the other one will repel the former [10, 12]. The charge also determines the magnitude of attraction or repulsion the better the objective function value, the higher the magnitude of attraction or repulsion [11]. There are four phases in EM algorithm: initialization of the algorithm, calculation of the total force, movement along the direction of the force and neighborhood search to exploit the local minima.

Initialize

Randomly select m points ($x_i = (x_i^1, x_i^2, \cdots, x_i^n)$, i = 1, 2, $\cdots$, m) from the feasible region as the initial particles. Distribute these initial particles randomly in the feasible field, then calculate the objective function value of every particle f (x_i), and note the particle whose current objective function value is the most optimized as x best.

$$x_t^B = \arg\max_{x_{i,t}\in S_t} \{f(x_{i,t})\} \tag{19}$$

Where x_t^B is the element of St that produces the maximum value in terms of the objective function.

Local search

Local search means to move a particle to its nearby optimum solution. Local search can be applied to all particles but it is time consuming so if it can be applied to current best particle there is an improvement in applying the local search. A simple search in electromagnetism like algorithm is also called the random line search. Random line search requires two parameters: δ and Local Search Iterations (LSITER). First, the maximum feasible step length rk at each dimension *k* is calculated as the product of δ and the range of dimension k (i.e. uk − lk). Then, for each particle *i*, this method searches along each dimension *k* for improvement of particle *i* for no more than LSITER times, each particle is searched according to its dimension with a proper step and when a best solution is found the search is terminated.

Calculate the resultant force

The calculation of the resultant force is the most significant step in the EM algorithm. The local and global information of the particles will be effectively combined together from this step. The superposition principle of the basic electromagnetic theory says that the electromagnetic force of one particle which is exerted by other particles is inversely proportional to the distance between particles and is directly proportional to the product of the amount of charge carried with them [11]. Firstly charge on each particle is calculated, on the basis of the $q_{i,t}$ the attractive or repulsive force is calculated on the i[th] particle. Through the calculation of the above equation, the particle with better optimized objective function value will have a larger amount of charge.

$$q_{i,t} = \exp\{-n\frac{f(x_{i,t}) - f(x_t^B)}{\sum_{j=1}^{N} f(x_{i,t}) - f(x_t^B)}\} \tag{20}$$

Force $F_{i.j}^t$ between two points $x_{i,t}$ and $x_{j,t}$ is calculated by:

$$F_{i,j}^t = \begin{cases} (x_{j,t} - x_{i,t})\dfrac{q_{i,t}.q_{j,t}}{\left\|x_{j,t} - x_{i,t}\right\|^2} if, f(x_{i,t}) > f(x_{j,t}) \\ (x_{i,t} - x_{j,t})\dfrac{q_{i,t}.q_{j,t}}{\left\|x_{j,t} - x_{i,t}\right\|^2} if, f(x_{i,t}) \le f(x_{j,t}) \end{cases} \tag{21}$$

Total force F_i^t corresponding to $x_{i,t}$ is calculated.

$$F_i^t = \sum_{j=1, j\neq i}^{N} F_{i,j}^t \tag{22}$$

According to this equation the value of force calculated for any two particles of the group, the particle which will have the larger optimized objective function value will attract the other one while the one with smaller objective function value will repulse the other one.

Move particles

After the force on particle is calculated it is moved in the resultant direction of the force with a random step size. Thus the position of each particle is updated accordingly after the completion of the iteration of the EM algorithm. The below defined equation defines that particles will move in certain direction where λ is between 0 and 1 also it is uniformly distributed, range is a vector whose components denote the allowed feasible movement toward the upper bound or the lower bound for the corresponding dimension.

$$x_{i,t} = x_{i,t} + \lambda\frac{F_i^t}{\left\|F_i^t\right\|}(Range) \quad \text{Where i=1,2…N} \tag{23}$$

According to electromagnetism theory for charged particles, each point in the search space is regarded as a charged particle and the charge of a point is found to be related to its objective function value. The points with better objective function value have more charges than other points, and according to the attraction-repulsion mechanism points with more charge attract other points in and points with less charge repel other points.

General scheme of EM algorithm

EM (N, LSITER, δ)
N – Population size
LSITER - max. No. of local search iterations
δ_t - Local search parameter
Initialize ()
While termination condition is not satisfied do
Local (LSITER, δ_t)
F= CalcF ()
Move (F)
End while

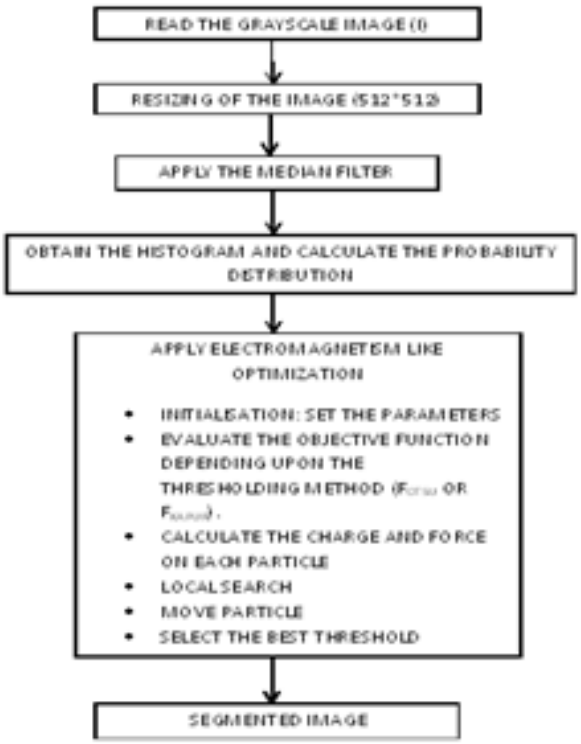

Fig. 1: Electromagnetism-like optimization algorithm

Harmony search optimization algorithm

Harmony search (HS) was first developed by Z.W. Geem et al. in 2001 [20], it is the new one in the category of metaheuristics. Its advantages have been used in various applications. It can be employed to solve many optimization problems including function optimization, engineering optimization, water distribution networks, groundwater modeling, and energy saving dispatch, truss design, vehicle routing, and many others [21, 22]. Harmony search is a music-based meta-heuristic optimization algorithm. Its quality is evaluated considering the objective functions that are employed by the Otsu's or Kapur's methods. The basic harmony search algorithm consists of three main phases: initialization, improvisation, and updating.

Initialization

In this step the harmony memory vectors are initialized. Let $x_i = \{x_i(1), x_i(2), \ldots x_i(n)\}$ represent the i^{th} randomly generated harmony vector.

$X_i(j) = l(j) + (u(j) - l(j))^* \text{ rand}(0,1)$ for j= 1,2,……..,n and i = 1, 2,…….……HMS

where: r and (0, 1) is matrix of random numbers between 0 and 1, u (j) and l (j) is the upper bound and lower bound respectively. Then HM matrix is filled with HMS vectors accordingly.

Improvisation

A new harmony vector X_{new} is built by applying the following three operators: memory consideration, random re-initialization, and pitch adjustment. Generating a new harmony is known as improvisation.

$$X_{new}(j) = \begin{cases} x_i(j) \in \{x_1(j), x_2(j), \ldots . x_{HMS}(j)\}, \\ \quad with \text{ probability HMCR}, \\ \{l(j) + u(j) - l(j)\} * rand(0,1), \\ \quad with\ probability \text{ 1- HMCR}. \end{cases} \quad (24)$$

where: HMCR is harmony memory consideration rate.

Every component obtained by memory consideration is further examined to determine whether it should be pitch adjusted. The pitch-adjusting rate (PAR) is defined as to assign the frequency of the adjustment and the bandwidth factor (BW) to control the local search around the selected elements of the HM. Hence, the pitch-adjusting decision is calculated as follows:

$$X_{new}(j) = \begin{cases} x_{new}(j) = x_{new}(j) \pm rand(0,1) * BW, \\ \quad \text{with probability PAR}, \\ x_{new}(j), \text{ with probability (1-PAR)}. \end{cases} \quad (25)$$

Updating the harmony memory

After a new harmony vector X_{new} is generated, the harmony memory is updated by the survival of the fit competition between X_{new} and the worst harmony vector X_w in the HM. Therefore X_{new} will replace X_w and become a new member of the HM in case the fitness value of X_{new} is better than the fitness value of X_w..

Harmony search algorithm

Step1: Set the parameters HMS, HMCR, PAR, BW, and NI.

Step2: Initialize the HM and calculate the objective function value of each harmony vector.

Step3: Improvise a new harmony X_{new} as follows:

for (j=1 to n) do

if(r_1< HMCR) then

$X_{new}(j) = X_a(j)$ where a ∈ (1,2,….,HMS)

If(r_2< PAR) then

$X_{new}(j) \pm r_3.BW$, where $r_1, r_2, r_3 \in$ r and (0, 1).

end if

if$X_{new}(j)$< l(j)

$X_{new}(j)$= l(j)

end if

if$X_{new}(j)$> u(j)

$X_{new}(j)$=u(j)

end if

else

$X_{new}(j)$= l(j)+ r.(u(j)-l(j)), where r ∈ r and (0,1)

end if

end for

Step4: Update the HM as $X_w = X_{new}$ if f (X_{new}) <f (X_w)

Step5: If NI is completed, the best harmony vector X_b in the HM is returned, otherwise go back to Step3.

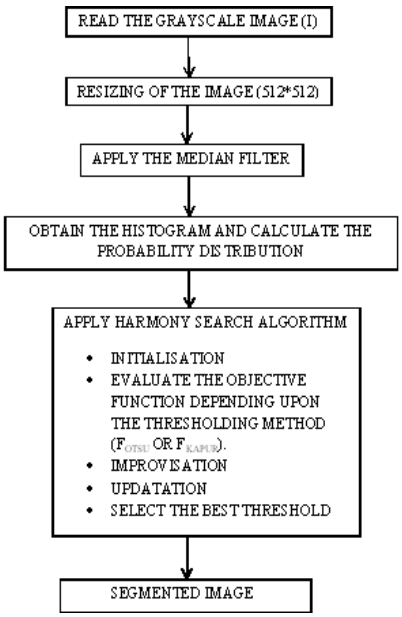

Fig. 2: Harmony search optimization algorithm

Results and Discussions

This section is divided into three parts. In the first part, the result of electromagnetism- like optimization algorithm is discussed. The second part consists of results obtained from harmony search optimization algorithm and the different processing steps are discussed. Finally, the comparisons between two methods are discussed.

Segmentation Results and Analysis

To demonstrate the effectiveness of the EMO and HS algorithm, the following two different objective functions are considered:

(i) Entropy (Kapur) based objective function

(ii) Between-class variance (Otsu) based objective function

The aim is to obtain the correct threshold values and higher objective values with fast computational ability. The results are obtained on 20 set of ultrasound kidney images. These images are called test images in our experiment. The ultrasound images found to be contaminated with the speckle noise. All the images have the same size 512*512 and are in JPGE format. These images are conditioned before applying segmentation. The images are subjected to median filter; median filter can remove the high frequency components from ultrasound images without disturbing the edges. Then the filtered output which is also known as preprocessed output is applied to the proposed algorithms. We have used two optimization algorithms i.e. electromagnetism-like optimization algorithm (EMO) and harmony search algorithm (HS). These are carried out over two objective functions: Otsu and Kapur entropy function. To illustrate the use of multilevel thresholding approach the segmentation is performed at different thresholds level. The results are determined at 2- level, 3-level, 4-level, and 5-level thresholds. Fig.3 and Fig.4 shows original and pre-processed images respectively.

Fig. 5 (a) shows the segmented images for test image 1 of EMO using Kapur as objective function at different level threshold values. The histogram shows the optimal threshold values at different levels. The objective function plot is the plot of objective value versus number of iterations. Fig. 5 (b) contains the results for test image 1 for EMO using Otsu as an objective function. Fig. 5 (c) is the result for test image 1 of

harmony search using Kapur as objective function. Fig. 5 (d) shows the results for test image 1 of harmony search using Otsu as objective function. Similarly all the results for remaining images have been shown in Fig. 6, Fig. 7, Fig. 8 and Fig. 9 respectively. The higher objective function value gives good segmentation results. It can be seen from the results that 5-level threshold segmentation gives better results as compared to 4-level and the others. In the analysis, both objective functions, Otsu's and Kapur's are employed to find the best threshold values for each image of the complete set of test images. When comparison is between EMO and HS, then for both the objective functions the EMO algorithm shows the better results. The EMO is found to be better in terms of segmentation when compared to other meta-heuristics algorithms [11]. The approach combines the good search capabilities of EMO algorithm with the use of some objective functions that have been proposed by the popular multilevel thresholding methods of Otsu and Kapur. The EMO method can effectively deliver the solution for complex optimization problems yet requiring a low number of iterations in comparison to other evolutionary methods [18].

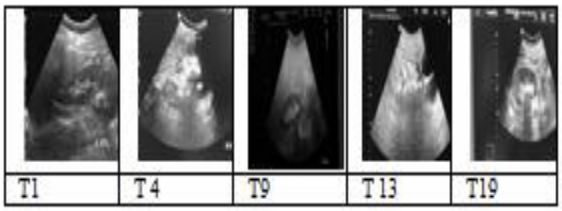

Fig. 3: Original images

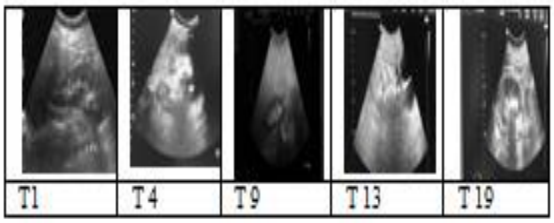

Fig. 4: Pre-processed images

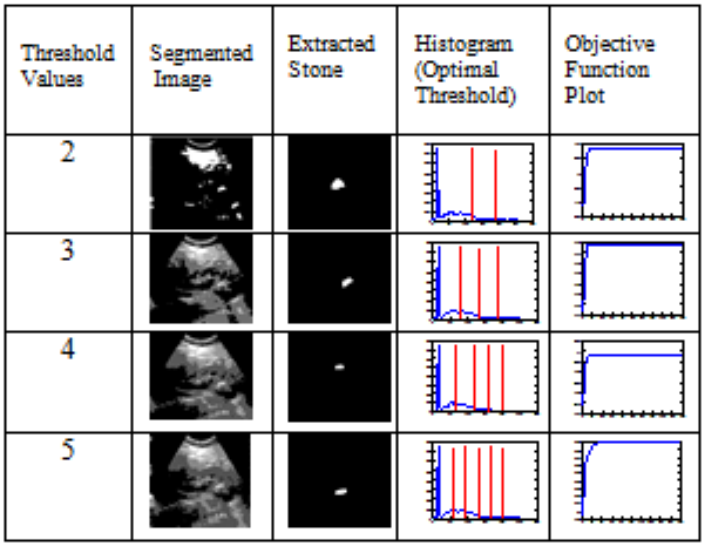

Fig. 5 (a): EMO (Kapur) for test image1

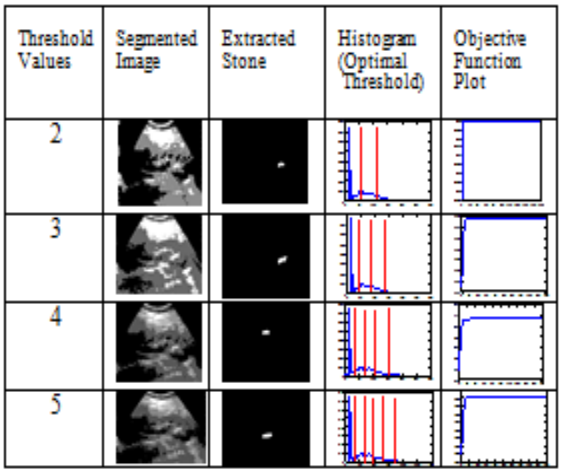

Fig. 5 (b): EMO (Otsu) for test image 1

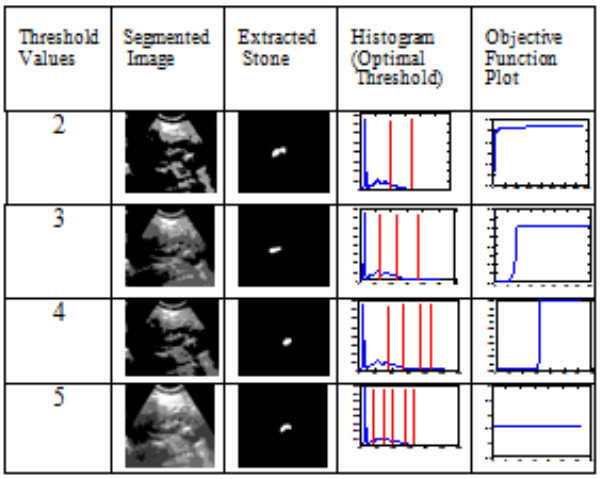

Fig. 5 (c): HS (Kapur) for test image1

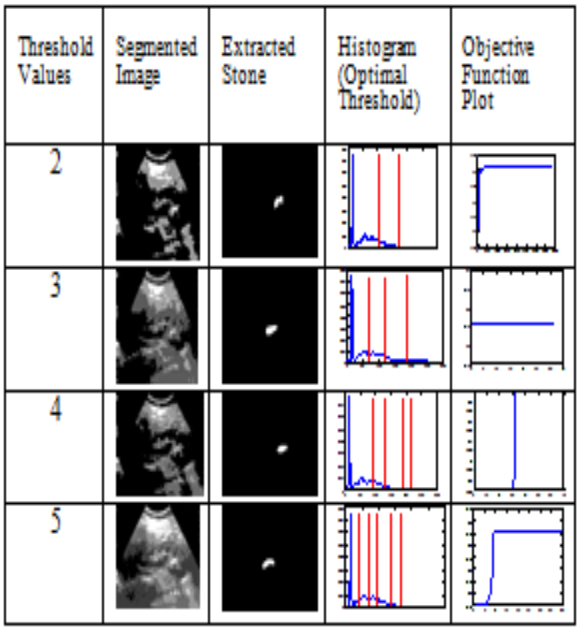

Fig. 5 (d): HS (Otsu) for test image 1

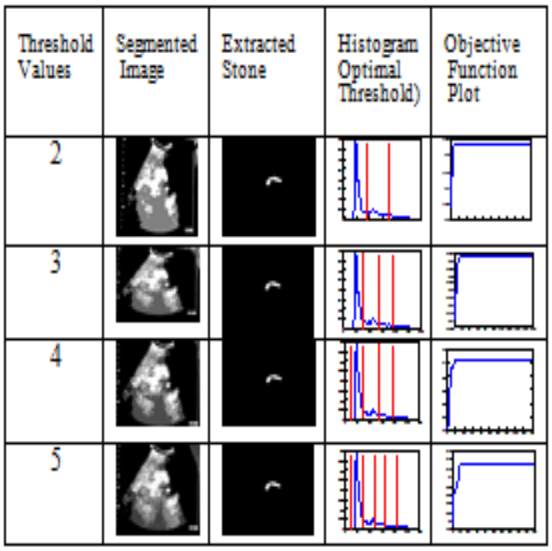

Fig. 6(a): EMO (Kapur) for test image 2

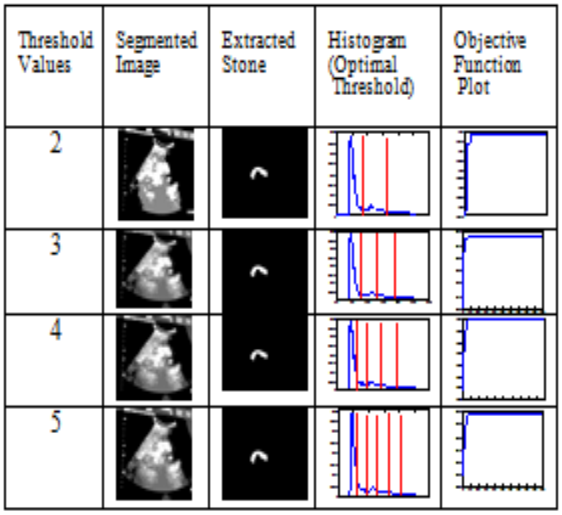

Fig. 6 (b): EMO (Otsu) for test image 2

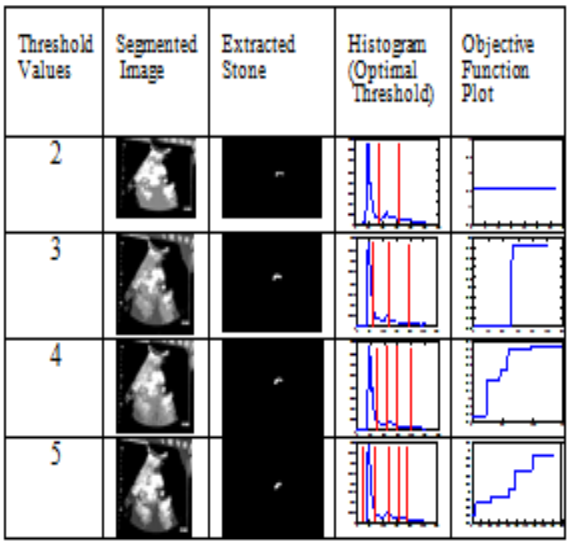

Fig. 6(c): HS (Kapur) for test image 2

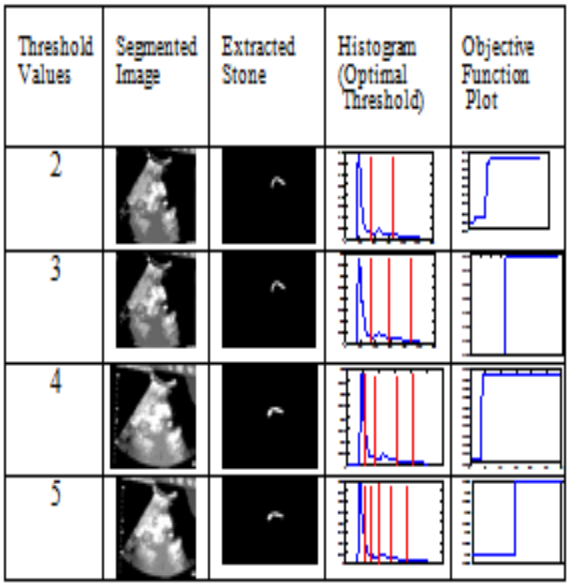

Fig. 6(d): HS (Otsu) for image 2

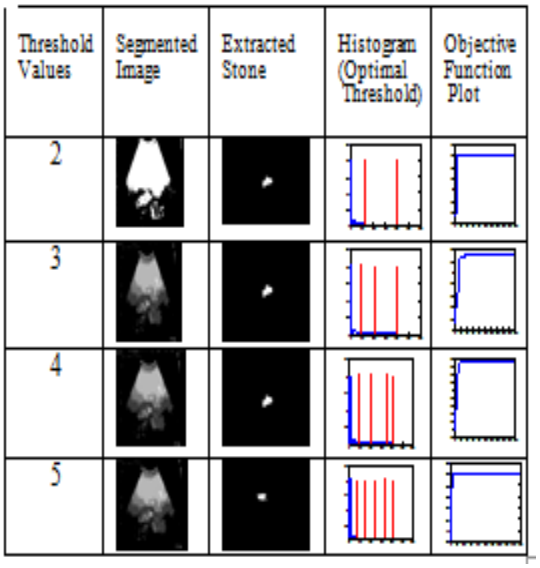

Fig .7 (a): EMO (Kapur) for test image 3

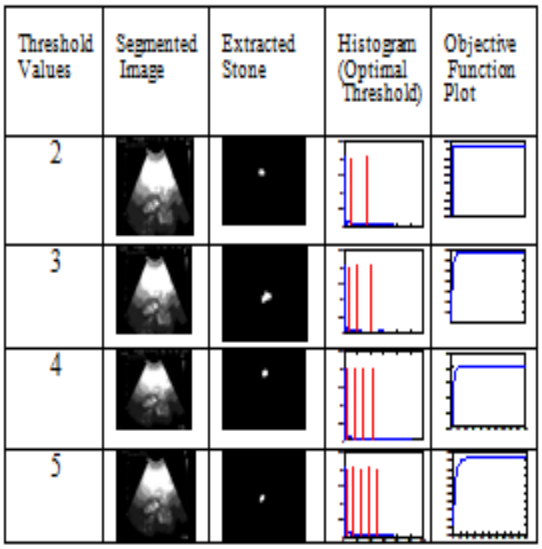

Fig. 7 (b): EMO (Otsu) for test image 3

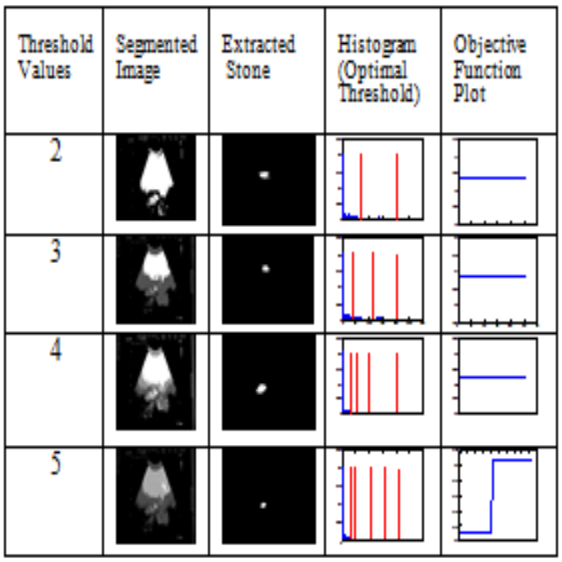

Fig. 7 (c): HS (Kapur) for test image 3

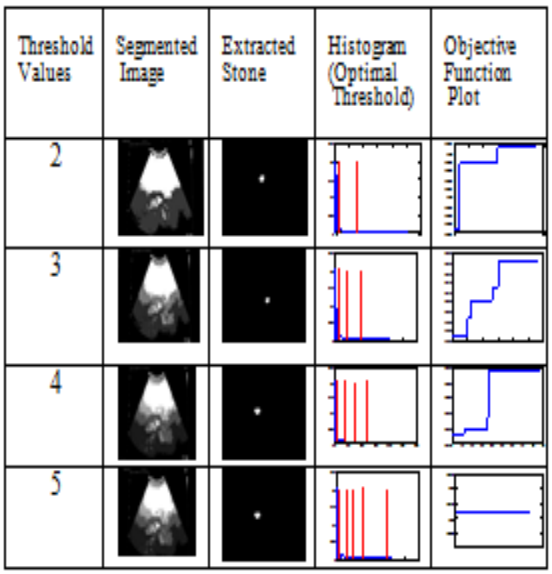

Fig. 7 (d): HS (Otsu) for test image 3

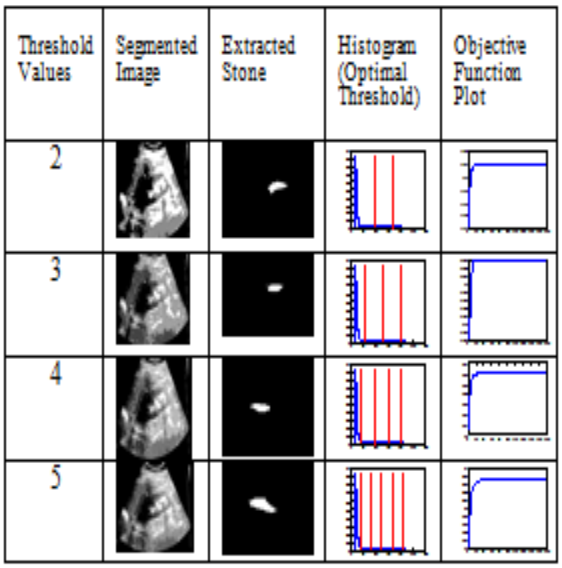

Fig. 8 (a): EMO (Kapur) for test image 4

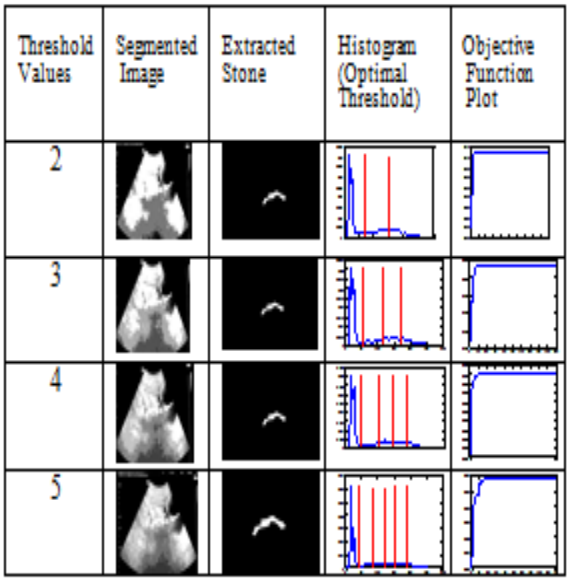

Fig. 8(b): EMO (Otsu) for test image 4

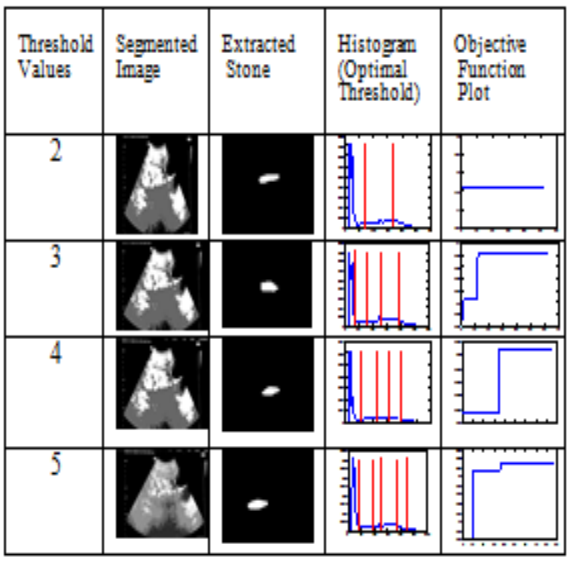

Fig. 8(c): HS (Kapur) for test image 4

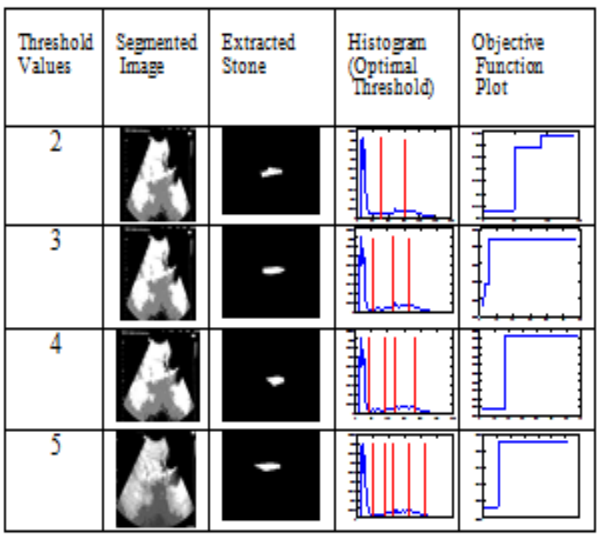

Fig. 8 (d): HS (Otsu) for test image 4

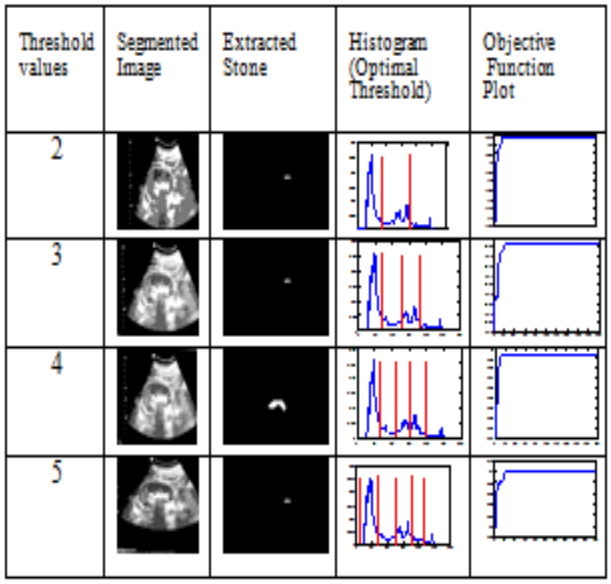

Fig. 9 (a): EMO (Kapur) for test image 5

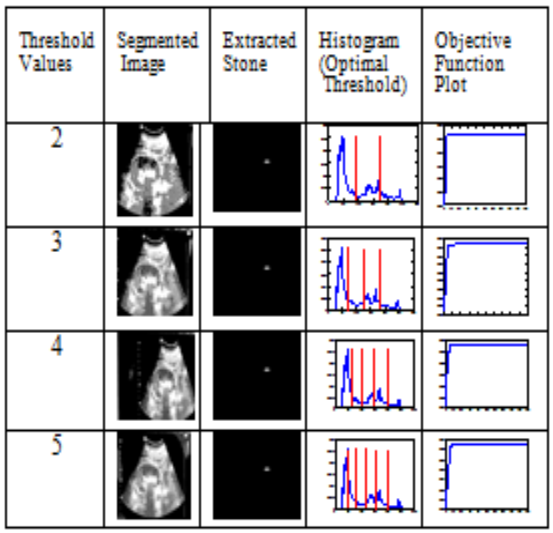

Fig. 9(b): EMO (Otsu) for test image 5

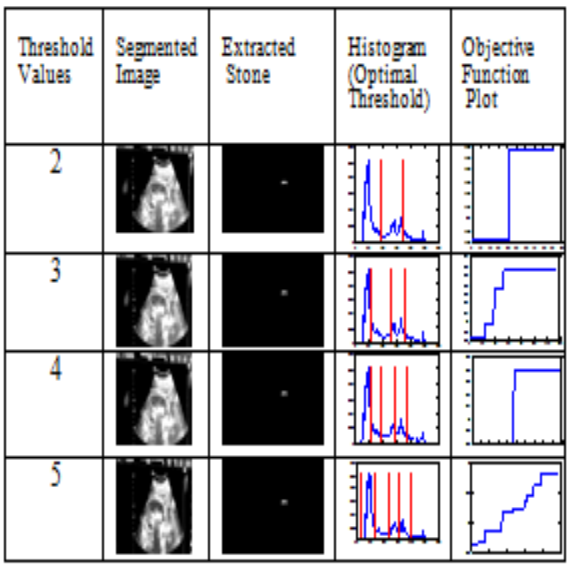

Fig. 9(c): HS (Kapur) for test image 5

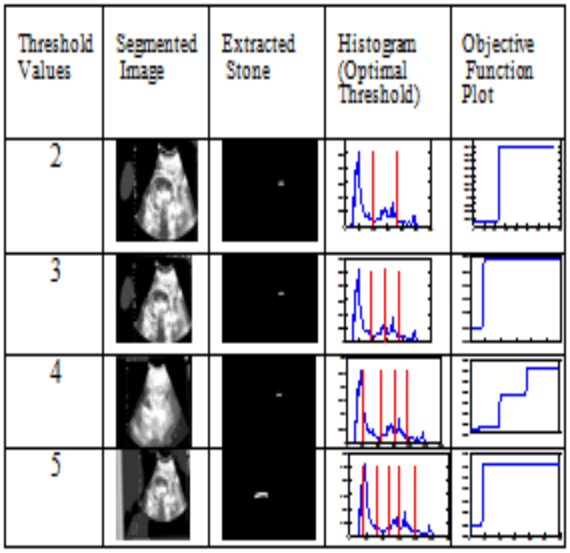

Fig. 9 (d): HS (Otsu) for test image 5

Since both the methods are stochastic, it is necessary to employ an appropriate statistical metrics to compare the efficiency of the algorithms. On the other hand, the peak-to-signal ratio (PSNR) is used to compare the similarity of an image (image segmented) against a reference image (original image) based on the mean square error (MSE) of each pixel. The MSE is the cumulative squared error between the segmented and the original image, whereas PSNR is a measure of the peak error. It is used as a standard mathematical model to measure an objective difference between two images. A lower value of MSE indicated less error and as seen in the inverse relation between MSE and PSNR, this translated to a high value of PSNR.

$$\text{PSNR} = 20\log_{10}\left(\frac{255}{RMSE}\right)_{\text{dB}}$$

$$\text{RMSE} = \sqrt{\frac{\sum\sum I_O(i,j) - I_S(i,j)}{M * N}}$$

where I_o is the original image and I_s is the segmented image.

The comparison of proposed methodologies can be done in two ways one is on the basis of objective function value. The higher the objective value, shown in Table 1 and Table 2, better the segmentation result [31, 30]. The other one is on basis of statistical values that is PSNR, MSE etc. The Table 3 shows the PSNR value which is compared in the next section.

Comparison of the two methods

The Table1 and Table 2 shows that the value of Kapur based EMO has larger value in each case as compared to Kapur based HS and Otsu based EMO has larger value as compared to Otsu based HS respectively for each case. Table 3 show the PSNR values for each case from the table it can be evidently seen that the Otsu based EMO and HS have higher value and also HS gives better PSNR value as compared to EMO. Higher the value of PSNR means good visual perception quality. Table 4 and Table 5 show the optimal thresholds value for both Kapur based EMO and HS and Otsu based EMO and HS. Table 6 shows the comparison of area of the radiologist expert and the area calculated using the proposed method. It is found that the EMO produces better results in terms of accuracy of area calculation.

Table 1: Comparison of objective values obtained by Kapur based objective function

Test Images	No. of Thresholds	Objective Values (Kapur)	
		EMO	HS
T1	2	18.0835	17.9129
	3	22.7760	22.5544
	4	26.9828	26.3499
	5	30.8994	29.5836
T2	2	17.3596	17.3096
	3	22.4825 26.9953 30.9660	22.2107
	4		26.5210
	5		30.4959
T3	2	17.9464	17.8381
	3	22.8190	22.3974
	4	27.2769	27.0173
	5	31.3418	30.5761
T4	2	17.8317	17.5351
	3	22.5267	22.1851
	4	27.0502	26.6286
	5	31.3110	30.8631
T5	2	18.0054	17.9233
	3	22.8844	22.1772
	4	27.3433	27.1479
	5	31.4612	30.2202
T6	2	18.0820	18.0640
	3	23.0395	22.3930
	4	27.2708	26.6765
	5	31.3978	30.2550
T7	2	15.4080	15.3421
	3	20.0192	19.7991
	4	24.4666	24.1238
	5	28.9260	28.1083
T8	2	15.8747	15.7337
	3	20.9622	20.2741
	4	25.3872	24.2867
	5	29.5342	28.7091
T9	2	16.5884	16.3673
	3	21.2958 25.6961	20.8663
	4	29.8729	24.2166
	5		27.8074
T10	2	17.6806	17.6390
	3	22.4169	22.1794
	4	26.7241	26.5794
	5	30.7276	30.4415
T11	2	17.9485	17.7752
	3	22.4949	22.3429
	4	26.8528	26.7835
	5	31.0328	30.4110
T12	2	17.5052	17.4279
	3	22.2319	22.1645
	4	26.8147	26.4089
	5	31.0210	29.8748
T13	2	17.2187	17.5730
	3	22.0583	22.3837
	4	26.6029	26.8239
	5	30.7378	30.2795
T14	2	17.5156	17.3878
	3	22.2333	22.2230
	4	26.8634	26.6934
	5	31.0948	30.5035
T15	2	17.7512	17.6321
	3	22.6472	22.2945
	4	27.0953	26.8449
	5	31.0509	29.9945

T16	2	16.7320	17.6858
	3	21.6147	22.3882
	4	26.2973	26.9792
	5	30.5364	30.6435
T17	2	17.4255 22.3284	17.3293
	3	26.8792	21.9770
	4	30.9915	26.3912
	5		30.0706
T18	2	17.4690	17.3108
	3	22.4096	21.7839
	4	26.9017	26.5656
	5	31.0223	30.6661
T19	2	18.1345	17.9563
	3	22.8607	22.5576
	4	26.9304	26.3856
	5	31.0065	30.8123
T20	2	17.3749	17.0294
	3	22.1500	21.7979
	4	26.8576	26.5891
	5	31.0407	30.3173

Table 2: Comparison of objective values obtained by Otsu based objective function

Test Images	No. of Threshold	Objective values (Otsu)	
		EMO	HS
T1	2	1.7389e+03	1.7289e+03
	3	1.8997e+03	1.8789e+03
	4	1.9695e+03	1.9606e+03
	5	2.0018e+03	1.9998e+03
T2	2	4.0153e+03	4.0141e+03
	3	4.1177e+03	4.1192e+03
	4	4.1746e+03	4.1656e+03
	5	4.2143e+03	4.1881e+03
T3	2	3.6368e+03	3.6322e+03
	3	3.7459e+03	3.7385e+03
	4	3.7984e+03	3.7918e+03
	5	3.8299e+03	3.8278e+03
T4	2	2.7119e+03	2.7110e+03
	3	2.8162e+03	2.8139e+03
	4	2.8700e+03	2.8490e+03
	5	2.8985e+03	2.8845e+03
T5	2	3.7880e+03	3.7841e+03
	3	3.9204e+03	3.9105e+03
	4	3.9918e+03	3.9901e+03
	5	4.0281e+03	4.0151e+03
T6	2	3.9593e+03	3.9543e+03
	3	4.0935e+03	4.0885e+03
	4	4.1670e+03	4.1574e+03
	5	4.1992e+03	4.1814e+03
T7	2	1.3061e+03	1.3011e+03
	3	1.3535e+03	1.3475e+03
	4	1.3759e+03	1.3625e+03
	5	1.3885e+03	1.3762e+03
T8	2	1.3866e+03	1.3861e+03
	3	1.4379e+03	1.4318e+03
	4	1.4634e+03	1.4527e+03
	5	1.4760e+03	1.4738e+03
T9	2	1.3681e+03	1.3561e+03
	3	1.4267e+03	1.4253e+03
	4	1.4502e+03	1.4492e+03
	5	1.4611e+03	1.4412e+03
T10	2	3.7167e+03	3.7129e+03
	3	3.8429e+03	3.8402e+03 3.8786e+03
	4	3.9024e+03	3.9217e+03
	5	3.9325e+03	

T11	2	3.6568e+03	3.6542e+03
	3	3.8131e+03	3.7880e+03
	4	3.8880e+03	3.8691e+03
	5	3.9287e+03	3.9159e+03
T12	2	3.9981e+03	3.9951e+03
	3	4.1440e+03	4.1402e+03
	4	4.2014e+03	4.2005e+03
	5	4.2316e+03	4.2206e+03
T13	2	4.2718e+03	4.2643e+03
	3	4.4037e+03	4.4021e+03
	4	4.4707e+03	4.4830e+03
	5	4.5035e+03	4.4879e+03
T14	2	4.1885e+03 4.3194e+03	4.1880e+03
	3	4.3829e+03	4.3012e+03
	4	4.4098e+03	4.3712e+03
	5		4.4017e+03
T15	2	3.4162e+03	3.4145e+03
	3	3.5143e+03	3.5054e+03
	4	3.5737e+03	3.5405e+03
	5	3.6029e+03	3.5715e+03
T16	2	3.9331e+03	3.9288e+03 4.0541e+03
	3	4.0572e+03	4.1108e+03
	4	4.1176e+03	4.1398e+03
	5	4.1484e+03	
T17	2	4.5379e+03	4.5355e+03
	3	4.6617e+03	4.6598e+03
	4	4.7192e+03	4.7095e+03
	5	4.7572e+03	4.7468e+03
T18	2	3.3649e+03	3.3625e+03
	3	3.4511e+03	3.4340e+03
	4	3.4977e+03	3.4784e+03
	5	3.5228e+03	3.5163e+03
T19	2	3.2864e+03	3.2777e+03
	3	3.4215e+03	3.4110e+03
	4	3.5030e+03	3.4856e+03
	5	3.5304e+03	3.5152e+03
T20	2	4.3483e+03	4.3476e+03
	3	4.4817e+03	4.4790e+03
	4	4.5452e+03	4.5435e+03
	5	4.5711e+03	4.5658e+03

Table 3: Comparison of PSNR value for both the methods

Test Images	No. of TH	EMO		HS	
		Kapur	Otsu	Kapur	Otsu
T1	2	13.4665	17.9231	14.2014	17.9539
	3	16.0434	20.1677	17.5872	19.4421
	4	17.7468	21.8170	15.1735	21.4891
	5	19.4265	22.8556	22.6011	22.8607
T2	2	15.4406 17.9874 19.8290	16.4846	15.6442	16.4662
	3	20.7740	18.8985	18.9922	18.8567
	4		19.8706	19.2478	19.7294
	5		21.0436	19.8423	20.3144
T3	2	16.2740	16.3900	16.1322	16.3234
	3	17.2405	17.7487	17.6658	17.6673
	4	18.5532	18.8039	18.6002	18.5454
	5	19.1608	19.7172	19.1114	19.3880
T4	2	14.0633	14.1205	14.1882	14.1058 15.0213
	3	15.1164	15.0638	15.4058	16.3381
	4	18.4728	16.0167	15.6265	16.7017
	5	19.5867	16.5940	18.8987	
T5	2	16.6421	16.9034	16.3978	16.7202
	3	18.4731	18.7735	18.0606	18.7208
	4	20.1102	20.3517	19.5255	20.3816
	5	21.1415	21.2415	19.2187	21.5743

T6	2	14.0815	15.8676	13.9533	15.9146
	3	17.2205	17.3097	16.8754	16.9341
	4	17.5887	18.8872	18.1618	18.3462
	5	18.7840	19.9365	18.3962	19.4915
T7	2	20.3001	23.0361	19.9916	23.1406
	3	20.6928	25.4165	23.7133	25.2306
	4	23.8026	27.2275	23.2564	26.0510
	5	23.8026	28.7334	25.1309	27.2931
T8	2	19.8135	22.6556	19.5373	22.4720
	3	19.8135	25.1120	22.2683	24.3423
	4	22.7750	26.9297	24.9448	25.7902
	5	22.8488	28.3662	20.9076	27.7384
T9	2	19.4259 22.9539	22.6168	19.7644 22.8772	21.9043
	3	22.9654	25.0115	24.4712	24.6565
	4	25.0383	27.0967	24.2834	27.0275
	5		28.8604		25.1852
T10	2	17.9376	18.0203 20.1998	17.6781	17.8517
	3	20.2536	21.8970	19.8834	20.2244
	4	21.8885	23.2753	21.5039	20.9903
	5	23.0763		22.9132	23.1035
T11	2	14.7609	16.8235	13.0555	16.6399
	3	20.2224	18.9701	18.6242	18.7828 20.5998
	4	18.6332	20.9317	19.9848	21.9378
	5	21.4413	22.1095	20.1747	
T12	2	16.2005	17.1316	17.1844	16.9517
	3	18.0433	19.1564	18.2173	18.9343
	4	19.5024	20.5599	20.1827	20.5325
	5	20.8936	21.5023	20.5276	21.1089
T13	2	16.7892	16.8887	15.7386	17.0551
	3	17.8393	18.9935	18.0291	19.0231
	4	19.9000	20.2385	19.5226	20.5764
	5	21.1658	21.1950	19.9629	20.5906
T14	2	14.0733	17.0381	16.3628	17.0184
	3	17.5023	19.3662	17.6291	19.3964
	4	20.6928	21.0540	20.5239	21.1378
	5	21.8491	22.4674	21.3776	22.4289
T15	2	14.3808 16.7136	15.7546	13.9676	15.5226
	3	17.8780 18.5694	16.9483	15.8600	16.8861
	4		18.4925	18.4518	17.9956
	5		18.9298	18.4834	18.1707
T16	2	13.9152	17.3962	17.2504	17.4454
	3	17.1227	19.3612	18.6738	19.3556
	4	19.5436	20.6768	20.4371	20.5699
	5	21.7588	21.7112	20.3983	21.5966
T17	2	16.7648	17.1769	16.4331	17.0673
	3	18.2540	19.1762	18.8141	19.0943
	4	20.0501	20.5069	19.0013	20.1283
	5	21.4289	21.5422	20.5880	21.1201
T18	2	15.8907	16.7715	14.2792	16.8049
	3	16.6523	17.8505	17.8213	17.9281
	4	18.3790	18.7551	17.2149	18.2718
	5	18.8611	19.2256	20.2889	19.8429
T19	2	13.7961	14.2071	14.2703	14.0331
	3	16.0299	15.9975	16.1743	15.4050
	4	16.9002	17.0833	16.8745	17.6995
	5	18.7312	18.6457	19.4806	20.5403
T20	2	14.8408	17.2530	15.3025	17.1530
	3	16.5932	19.5680	18.6120	19.2357
	4	20.0878 21.6325	20.9946	19.9133	20.9824
	5		22.3495	20.8067	21.7970

Table 4: Optimal threshold values obtained by Kapur based method

Images	No. of Threshold	Threshold values(kapur)	
		EMO	HS
T1	2	105, 179	97, 171
	3	82 ,135,191	67,119,187
	4	69,117,159,199	90,131,187,214
	5	60, 96, 131 ,167, 203	39 ,70, 98 , 139,165
T2	2	60, 160	68,169
	3	50,110, 195	57,110,163
	4	50,109,157 205	41, 83,140,210
	5	37 ,73 ,110 158, 205	42,66,101 160 211
T3	2	65 ,153	52,143
	3	60,131 ,201	62,112,160
	4	51 ,103,154,207	55,95,143,193
	5	51 92 133 174 215	50,69,109 152,196
T4	2	88, 174	84, 157
	3	74 , 135, 194	64, 119, 197
	4	23, 74, 135 ,194	74,109,149,198
	5	23, 69, 117 ,162, 209	21, 66,124 156 , 191
T5	2	66 , 161	102, 176
	3	53, 122 , 191	51 104 138
	4	41 96 149 202	59 114 167 211
	5	40, 83, 126 170, 212	37, 65, 96 120 218
T6	2	72, 180	70, 181
	3	71,128,187	57,111, 190
	4	71,127, 178 218	66, 131,165 207
	5	53, 89, 129 179 218	62, 90,113 138,183
T7	2	64 170	55, 169
	3	57 137 177 46 92 139 177	43,92,152
	4	46 92 139 177 234	51,86,147,172
	5		39,85,119 144, 176
T8	2	67 152	81, 153
	3	67 152 222	56, 102,153
	4	50 98 156 222	36,72,110 158
	5	50 97 149 185 222	65,119,163 193,225
T9	2	59, 202	68, 202
	3	45,101,202	36,113,205
	4	45,101,176, 202	32,57,98, 204
	5	37 , 76 ,118 176 , 202	34,46,103 156, 211
T10	2	59 147	48,139
	3	46 108 170	49 ,93, 148
	4	39 86 135 184	53,96,143 181
	5	34 71 111 152 193	19, 70,109 151, 187
T11	2	107 177	129 189
	3	67 128 187	78, 126,171
	4	36 86 141 195	37, 77 ,140 191
	5	34 77 122 167 211	51, 71,133 174,206
T12	2	97 , 172	77 ,149
	3	74,139,205	39,113,178
	4	36 ,93 ,149 206	59,109,154 199
	5	34 79 124 169 214	50,75,119 174, 215
T13	2	92 167	69,171
	3	53,124,197	47,95,174
	4	40 ,94,148 203	36,76, 131 192
	5	37 ,81,123 166 ,210	39,96,128 188,223
T14	2	122 185	51, 148
	3	40 125 187	41,125,190
	4	29 75 129 190	31, 89,138, 200
	5	29 75 123 165 209	39,81,128 161,189
T15	2	72 179	60, 176
	3	67 137 200	75 ,110,205
	4	57,110,162 209	48, 111,155 200
	5	56 103 142 180 217	49, 96 ,131 146 ,216
T16	2	131 204	59, 147
	3	26 98 191	68,127,202
	4	26 89 153 208	37,84,139 196
	5	25 79 124 168 210	31,54, 86 129 ,205

T17	2	58 150	63, 162
	3	48 123 196	45,94,155
	4	36 92 149 205	43 ,88 ,121 ,199
	5	35 78 123 165 208	48 ,78 ,103 162, 192
T18	2	117 206	122 ,187
	3	52 129 206	50 ,105,165
	4	52 101 152 209	58,105,177 218
	5	52 96 140 182 216	19 ,44, 107 167,217
T19	2	85 179	94, 170 61,131,179
	3	70 126 184	60 ,93,143 186
	4	66 112 154 200	16 ,65,120 155,195
	5	16 70 126 179 215	
T20	2	121 191	61 ,169
	3	30 84 183	36,83, 154
	4	31 83 144 201	34 ,74, 139 191
	5	30 82 129 172 212	33 ,66,128 167, 197

Table 5: Optimal threshold values obtained by Otsu based method

Images	No. of threshold	Threshold values(Otsu)	
		EMO	HS
T1	2	52, 111	44, 101
	3	41, 83 , 136	27, 74, 136
	4	36,71,105, 152	38 ,67 ,112 159
	5	35 67 95 127 171	33, 64, 91 ,123 ,176
T2	2	77 160	75 157
	3	50,106,166	64,125,175
	4	47 99 147 191	57, 113,160 202
	5	40 83 126 161 201	59 , 83, 127 150 ,194
T3	2	73 151	66 149
	3	61 120 177	57 ,107, 176
	4	50, 94 142 188	54 ,108, 159 200
	5	42 77 120 161 201	47 ,89, 128 170 209
T4	2	88 163	89, 167
	3	78,131,188	80, 126, 184
	4	65,101,145 196	58 , 88, 156 204
	5	61 92 128 165 207	59, 82, 103 142 , 187
T5	2	68 152	63, 153
	3	55, 116,176	53, 112,161
	4	40 84 132 185	37 , 85, 131 187
	5	38 ,78 ,120 160 203	29, 66, 89 133, 191
T6	2	84 161	78 154
	3	56,117 ,184	57 112 190
	4	48,99, 151 195	58 96 146 194
	5	43 ,76, 118 156 197	37 59 99 164 206
T7	2	26 79	27 88
	3	20 57 100	24 51 90
	4	15 41 74 110	23 55 90 142
	5	12 , 32 58 87 117	19 45 69 106 166
T8	2	27 79	25 77
	3	19 ,52, 93	13 55 91
	4	16 43 75 108	13 30 62 89
	5	14 36 60 88 116	13 40 66 94 127
T9	2	27 87	17 79
	3	16 51 102	16 46 97
	4	14 38 71 113	12 37 76 117
	5	13 34 61 94 126	10 36 56 96 185
T10	2	60 143	54 142
	3	40 96 161	47 100 163
	4	33 77 126 176	27 55 94 166
	5	25 55 94 136 180	25 73 104 137 186
T11	2	61 139	57 138
	3	52,110,164	48 102 143
	4	40 83 125 173	44 88 116 157
	5	37 76 112 148 188	42 74 105 129 173
T12	2	62 139	57 136
	3	54,113,167	47 112 164
	4	47,94,136 179	44 92 134 176
	5	44 ,85,121 156 , 191	45 91 119 141 189

T13	2	70 149	78 151
	3	54,113,168	55 113 164
	4	48 99 145 188	45 90 125 182
	5	43 ,86, 125 160 197	50 86 110 160 212
T14	2	61 158	61 155
	3	49,106, 174	56 93 170
	4	45,94, 138 195	51 94 155 200
	5	34, 70 , 103 143 198	27 65 100 154 212
T15	2	84 159	82 163
	3	74,134,181	83 141 191
	4	49 ,91, 139 183	42 , 110, 146, 182
	5	48 89 134 168 204	58 , 85, 125 164 , 177
T16	2	64 147	68 , 154
	3	51,111, 171	57 , 112, 173
	4	43 92 141 188	50 , 98 , 136, 189
	5	38 76 115 154 195	31 , 77, 125 154 , 194
T17	2	70 151	64 , 147
	3	53 115 172	49, 109, 169
	4	41 88 138 185	48 , 85, 147, 186
	5	38 77 118 157 196	33 ,68, 115 167 , 195
T18	2	71 140	75 , 138
	3	66 124 169	53, 99, 156
	4	57 101 141 181	74, 126, 154 192
	5	55 95 130 160 192	38, 63,99, 135, 185
T19	2	95 173	102, 186
	3	70 124 185	88, 139, 188,
	4	61 105 151 198	53, 109, 150, 189
	5	50 76 114 153 199	42, 81, 122, 150, 197
T20	2	64 144	61, 142
	3	53,115,167	60, 127, 175
	4	50,104,145 187	47, 97, 139, 182
	5	36 75 113 150 190	30, 63, 113, 151, 197

Table 6: Segmentation performance

Test Images	Radiologist Expert (mm^2)	Kidney stone Area(mm^2)		Error of this method	
		EMO	HS	EMO	HS
T1	46.69	45.95	43.87	0.74	3.09
T2	37.21	36.76	34.09	0.45	3.12
T3	106.09	103.89	104.45	2.20	1.64
T4	441	435.04	423.87	5.96	17.13
T5	55.09	53.72	53.64	1.37	1.45
T6	25	22.05	21.33	2.95	3.67
T7	22.53	20.09	18.46	2.44	4.07
T8	23.32	20.72	21.98	2.60	1.34
T9	166.41	164.09	163.78	2.32	2.63
T10	376.36	374.52	370.23	1.84	6.13
T11	39.27	39.11	36.32	0.16	2.95
T12	153.76	150.82	151.09	2.94	2.67
T13	1232.01	1220.46	1221.54	11.55	10.47
T14	15.21	14.92	13.98	0.29	1.23
T15	256	243.21	240.87	12.79	15.13
T16	533.6	529.54	525.63	4.06	7.97
T17	462.4	458.02	453.49	4.38	8.91
T18	25	23.09	20.92	1.91	4.08
T19	225	222.83	219.42	2.7	5.58
T20	17.64	17.03	14.09	0.61	3.55

Conclusions

The proposed algorithms are tested on 20 set of kidney stone ultrasound images. Both the algorithms EMO and HS have been compared with each other with two objective functions: Kapur and Otsu respectively. From the value of the objective function it is evident that the electro-magnetism like optimization algorithm with Otsu based objective function shows higher value. The higher the objective value the better the segmentation result. For both the algorithms Otsu based objective function shows the higher value as compared to Kapur based objective function. To qualify the segmentation results, the kidney stone images are segmented with various threshold levels (m= 2, 3, 4, 5). The quality of the segmentation is better when the number of thresholds m=5 is chosen. It can also be evidently seen from the value of optimal threshold that Otsu based EMO is better for segmentation quality. The other metric used to compare the segmented image and the original image is the peak signal to-noise-ratio (PSNR) value. The PSNR is a measure of the peak error. It is used as a standard mathematical model to measure an objective difference between two images. The higher value of PSNR means the higher quality of image, the objective measures are particularly good at predicting human visual response to image quality and less error is introduced in the image. The PSNR value of the Kapur based EMO is higher than the Kapur based HS and for Otsu based objective function also EMO algorithm shows higher image quality. The segmented stone area is calculated and compared with the stone area marked by the expert radiologist. The relative error is also calculated, which shows the accuracy obtained by each method. Further work is in progress to test a hybrid approach of EMO and HS with active contour to improve the accuracy of segmentation.

References

[1] M. Maitra, and A. Chatterjee, “A hybrid cooperative comprehensive learning based PSO algorithm for image segmentation using multilevel thresholding”, Expert Systems with Applications, vol. 34, pp. 1341-1350, 2008.

[2] P. K. Sahoo, S. Soltani and A. K. C. Wong, “A survey of thresholding techniques”, Computer Vision, Graphics and Image Processing, vol. 41, no. 2, pp. 233-260, 1988.

[3] N. Otsu, “A threshold selection method from gray level histograms,” IEEE Transaction on Systems, Man and Cybernetics, vol. 9, no. 1, pp. 62-66, 1979.

[4] S. Dasgupta and S. Das “Bacterial foraging optimization algorithm: theoretical foundations, Analysis, and Applications” Studies in Computational intelligence, vol. 203, pp. 23-55, 2009.

[5] K. M. Passino, “Biomimicry for optimization, control, automation” Springer-Verlag London, UK, 2005.

[6] R. C. Gonzalez and R. E. Woods, Digital Image Processing, edition 2, Addison Wesley, 1992.

[7] J. Kittler and J. Illingworth, “Minimum error thresholding,” Pattern Recognition., vol. 19, no. 1, pp. 41–47, 1986.

[8] S. Binitha and S. S. Sathya, “A survey of bio inspired optimization algorithms”, International Journal of Soft Computing and Engineering, vol.2, pp. 2231–2307 Issue-2, May 2012.

[9] S. İ. Birbil and S-Cherng Fang “An electromagnetism-like mechanism for global optimization”, Journal of Global Optimization, vol. 25, pp. 263–282, 2003.

[10] D. Olivaa, E. Cuevas, G. Pajares, D. Zaldivar and V. Osuna, “A multilevel thresholding algorithm using electromagnetism optimization”, Neurocomputing, vol. 139, pp. 357-381, 2014.

[11] L. dos S. Coelho and P. Alotto, “Multi objective electromagnetic optimization based on a non-dominated sorting genetic approach with a chaotic crossover operator”, IEEE Transactions on magnetic, vol. 44, no. 6, June 2008

[12] C. Zhang, Xi. Li, L. Gao and Q. Wu, “An improved electromagnetism-like mechanism algorithm for constrained optimization”, Expert Systems with Applications, vol. 40, pp. 5621-5634, 2013.

[13] Wan M. Hafizah, Eko Supriyanto, “Automatic generation of region of interest for kidney ultrasound images using texture analysis”, International Journal of Biology and Biomedical Engineering, issue 1, vol. 6, pp.1289-1305, 2012.

[14] P. R. Tamilselvi, “Detection of renal calculi using semi-automatic segmentation approach”, International Journal of Engineering Science and Innovative Technology (IJESIT), vol. 2, issue 3, pp. 547-552, May 2013

[15] Miao Miao and Jianguo Jiang, “Electromagnetism-like mechanism algorithm based on normalization and adaptive move operator”, Journal of Computational Information Systems, vol. 8, no. 18, pp. 7449–7455, 2012.

[16] P. R. Tamilselvi and P. Thangaraj, "An Efficient segmentation of calculi from US renal calculi images using ANFIS System", European Journal of Scientific Research, vol. 55, no. 2, pp. 323-333, 2011.

[17] Tamilselvi and Thangaraj, “Computer aided diagnosis system for stone detection and early detection of kidney stones", Journal of Computer Science, vol. 7, No. 2, pp. 250-254, 2011.

[18] C. T. Su and H. C. Lin, “Applying electromagnetism-like mechanism for feature selection,” Information Sciences, vol. 181, no. 5, pp. 972-986, 2011.

[19] K. Hammouche, M. Diaf and P. Siarry, “A comparative study of various meta-heuristic techniques applied to the multilevel thresholding problem”, Journal of Engineering Applications of Artificial Intelligence, vol. 23, no. 5, pp. 676-688, 2010.

[20] D. Oliva, E. Cuevas, G. Pajares, D. Zaldivar, and M. Perez-Cisneros, “Multilevel thresholding segmentation based on harmony search optimization”, Journal of Applied Mathematics, vol. 2013, pp.4348-4366, 2013.

[21] E. Cuevas, N. Ortega-S. anchez, D. Zaldivar, and M. Perez-Cisneros, “Circle detection by harmony search optimization”, Journal of Intelligent and Robotic Systems, vol. 66, pp. 1–18, 2011.

[22] O. M. Alia and R. Mandava, “The variants of the harmony search algorithm: an overview,” Artificial Intelligence Review, vol. 36, no. 1, pp. 49–68, 2011.

[23]X.-S. Yang, “Harmony Search as a metaheuristic algorithmin: music-inspired harmony search algorithm: Theory and Applications”, Studies in Computational Intelligence, Springer Berlin, vol. 191, pp. 1-14, 2009.

[24] S. H. Cho, H. T. Duy, J. W. Han and H. Hwang, “Multi-level thresholding based on non-parametric approaches for fast segmentation”, Journal of Biosystems Engineering, vol. 38, no. 2, pp. 234-240, 2013.

[25]Jun-Lin Lin, Chien-Hao Wu and Hsin-Yi Chung, “Performance comparison of electromagnetism-like algorithms for global optimization”, Applied Mathematics, pp. 1265-1275, issue 3, 2012.

[26] A. I. Ahamed, B. M. F. Basha and M. M. Surputheen, “Renal calculi detection in ultrasound images and diagnosis of images using image segmentation”, IOSR Journal of Computer Engineering, vol. 16, issue 3, 2014.

[27] S. Xie and H. Nie, "Retinal vascular image segmentation using genetic algorithm plus FCM clustering", in proceedings of the 3rd International Conference on Intelligent System Design and Engineering Applications, pp. 1225-1228, 2013.
[28] A. Sheta, M. S. Braik , S. Aljahdali ,"Genetic Algorithms: A tool for image segmentation" International Conference on Multimedia Computing and Systems (ICMCS) IEEE, pp.84- 90, May 2012.
[29] K. K. Singh, A. Singh, "A study of image segmentation algorithms for different types of images", International Journal of Computer Science Issues, vol. 7, issue 5, pp.no. 414-417, September 2010.
[30] P. D. Sathya, R. Kayalvizhi, "Optimal segmentation of brain MRI based on adaptive bacterial foraging algorithm", Journal of Neurocomputing, vol. 74, pp. 2299–2313, 2011.
[31] P. D. Sathya, R. Kayalvizhi, "Modified bacterial foraging algorithm based multilevel thresholdingfor image segmentation", Journal of Engineering Applications of Artificial Intelligence, vol. 24, pp. 595–615, 2011.
[32] www.google.com
[33] www.wikipedia.com
[34] www.medicinenet.com
[35] www.emedicinehealth.com
[36] www.healthline.com